frontiers | Frontiers in Energy Research

ORIGINAL RESEARCH
published: 10 May 2022
doi: 10.3389/fenrg.2022.888389

Energy Transformation and Entropy Investigation in the Nanofluid Composed by γ-Nanomaterial Over a Permeable Convective Surface With Solar Thermal Radiation: A Numerical Analysis

Adnan[1], Waqas Ashraf[2], Hafiz Junaid Anjum[3], Ilyas Khan[4], Mohamed Mousa[5] and Sadok Mehrez[6,7]*

[1]Department of Mathematics, Mohi-ud-Din Islamic University, Nerian Sharif AJ&K, Pakistan, [2]Department of Applied Mathematics and Statistics (AM&S), Institute of Space Technology (IST), Islamabad, Pakistan, [3]Department of Mathematics, COMSATS University Islamabad, Islamabad, Pakistan, [4]Department of Mathematics, College of Science Al-Zulfi, Majmaah University, Al-Majmaah, Saudi Arabia, [5]Electrical Engineering, Faculty of Engineering and Technology, Future University in Egypt, New Cairo, Egypt, [6]Department of Mechanical Engineering, College of Engineering at Al Kharj, Prince Sattam Bin Abdulaziz University, Al-Kharj, Saudi Arabia, [7]Department of Mechanical Engineering, University of Tunis El Manar, ENIT, Tunis, Tunisia

OPEN ACCESS

Edited by:
Hsien-Yi (Sam) Hsu,
City University of Hong Kong, Hong Kong SAR, China

Reviewed by:
Gireesha B. J.,
Kuvempu University, India
Iskander Tlili,
King Saud University, Saudi Arabia

***Correspondence:**
Adnan
adnan_abbasi89@yahoo.com

Specialty section:
This article was submitted to Solar Energy, a section of the journal Frontiers in Energy Research

Received: *02 March 2022*
Accepted: *06 April 2022*
Published: *10 May 2022*

Citation:
Adnan, Ashraf W, Junaid Anjum H, Khan I, Mousa M and Mehrez S (2022) Energy Transformation and Entropy Investigation in the Nanofluid Composed by γ-Nanomaterial Over a Permeable Convective Surface With Solar Thermal Radiation: A Numerical Analysis. Front. Energy Res. 10:888389. doi: 10.3389/fenrg.2022.888389

The modern world moves toward new inventions by using nanotechnology and solar thermal radiations. On Earth, the Sun is the leading source of solar energy having a wider range of applications. These can be found in solar power plates (SPP), photovoltaic cells (PVC), solar thermal aircraft, and photovoltaic lighting. Therefore, the study is organized to analyze and improve the energy efficiency in the nanofluid over a permeable convective surface. The used nanofluid is synthesized by γ-nanoparticles and water. A theoretical experiment is conducted and a constitutive relation for the momentum and energy modeled. The model was tackled numerically and obtained the results for the velocity and energy transformation under varying effects of the pertinent flow parameters. From the study, it is observed that energy efficiency of the surface could be improved in the presence of solar thermal radiations, viscous dissipation, and convective heat conduction.

Keywords: γAl_2O_3 nanoparticles, solar thermal radiations, convective heat condition, numerical analysis, viscous dissipation

1 INTRODUCTION

The solar thermal radiations are the leading source of solar energy which has paramount importance in the modern technological world. It has wider applications in aerospace sciences, paint industries, electronics, and biomedical engineering. To enhance thermal energy, several conventional solar power plants were established. Although their prices and efficiencies are not human-friendly, yet, with the passage of time, these become more effective by inducing modern technologies in the solar plants regarding their thermal performance. The utilization of solar thermal radiation in the power plant industries remains a well-intentioned motive of the researchers and scientists. Execution of the power generation system and exergy analysis was reported by Wu et al. (2020). In 2021, Benhadji Serradj et al. (2021) discussed the design and

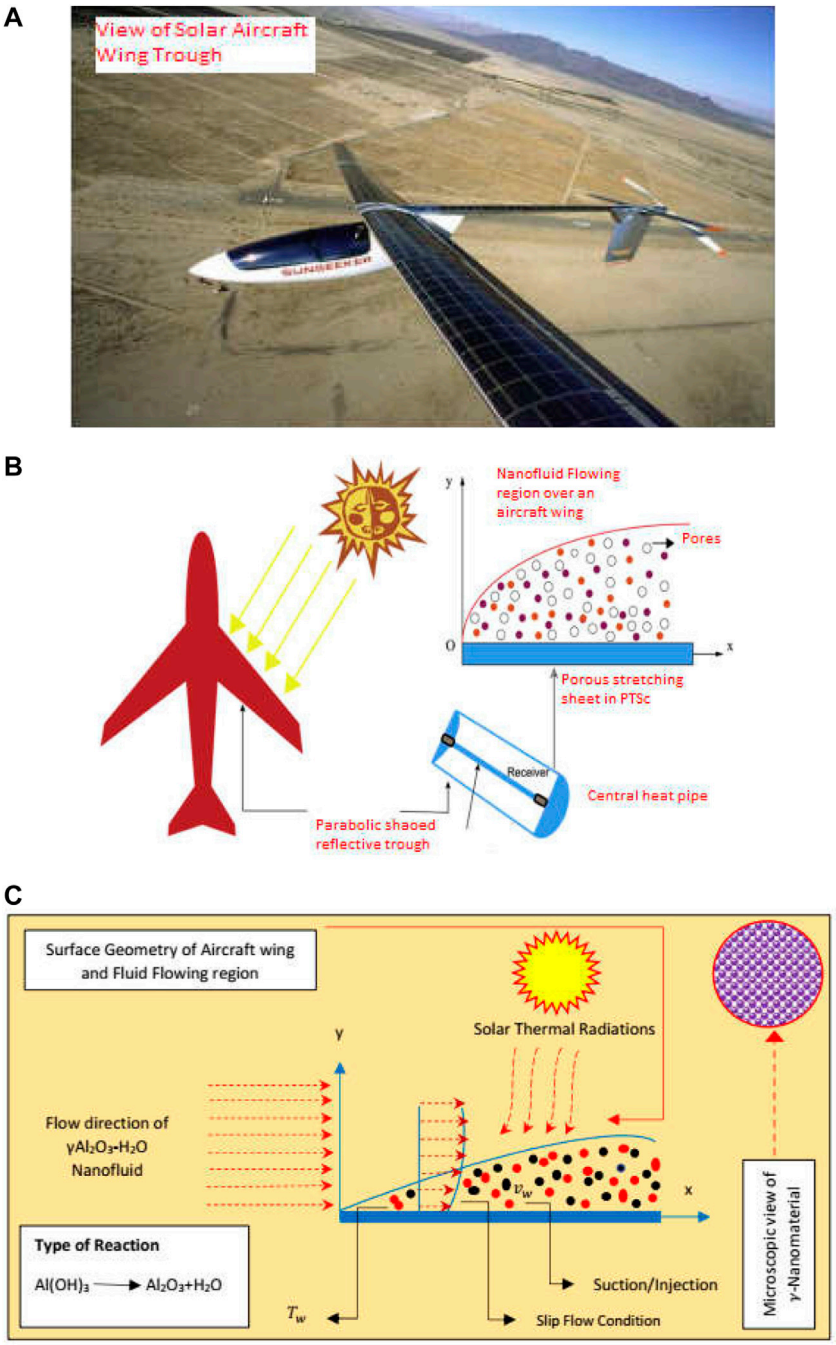

FIGURE 1 | (A) Schematic of the solar aircraft. **(B)** Theoretical experimental setup for a surface. **(C)** Flow schematic of the nanofluid over a permeable surface.

performance of the parabolic trough collector plant. Utilization of the hybrid random vector for the optimized model was reported by Zayed et al. (2021).

The unrestricted approachability of solar thermal energy points innovative green technology appearance very talented concerning affordability, sustainability, protection, and spotless means of transportation. To build a solar aircraft that has much ability of energy storage through solar-powered aircraft technique contains photo-voltaic cells, rechargeable batteries, and a maximum power point tracker. These cells joined with trough of aircraft wing through which solar energy transforms into electrical energy and then is utilized to enhance the efficiency of the aircraft force system and avionics. A Swiss aeronaut, Bertrand Piccard, and a professional pilot, Andre Borschberg, significantly contributed to the development of solar aircraft. After their untiring efforts, finally they built fuel-less and

environment-friendly aircraft consisting of a single seat. The major characteristic of the aircraft is solar energy playing the role of fuel for structured aircraft, due to which it is pollution free.

For said purpose, the aircraft is designed in such a way that photovoltaic cells adjusted under the craft wings act as the source of power for electric motors. Finally, the propellers in rotation gained mechanical energy produced by the motors and attained the desired kinetic energy. A historical perspective and future challenges in solar base airplanes were examined by Zhu et al. (2014). The study related to solar aircraft systems is discussed in the study by Abbe and Smith (2016). Furthermore, a comprehensive review for various methods to extract energy for solar aircraft was described by Gao et al. (2015). The flight efficiency of solar aircraft primarily depends on the power relevant to suitably choosing PV cells and weight. In order to achieve higher efficiency of solar aircraft, various technologies and materials have been examined. The aero dynamists are still working to improve the efficiency of solar aircraft by modifying PV cells. It is interesting to know that it utilized the Sun as an energy source in day-time and provided energy to the schemes at night-time. The schematic of the solar aircraft is depicted in **Figure 1A**.

In the designing of solar aircraft, parabolic trough solar collector (PTSC) is the most imperative skill; so far, they broadly used the other-directed solar power systems. Some imperative investigations of improved efficiency of solar aircraft associated with latest modern world technologies were described by Malan and Kumar (2021) and Goudarzi et al. (2020), respectively. In the organized study, our core concern will be the analysis of solar thermal efficiency of aircraft (STA). Thermal performance for the parabolic trough collector was explored in the study by Mwesigye and Yılmaz (2020). Another comparative investigation for three different solar aircraft was discussed in the study by Atiz (2020). An experimental study for parabolic collectors with direct flow was reported by Rezaeian et al. (2021).

Thermodynamics featuring in solar instruments can be improved effectively through nanoliquids coating. In which one of the significant ways is to induce nanofluid with functioning fluid due to which thermal performance of the device becomes progressive. Lately, researchers observed that the efficiency of solar refrigeration structure (SRS), solar devices (SDs), and water heater solar cells (WHSCs) may be upturned if the nanomaterials of high thermal conductance are utilized in the manufacturing of aforementioned modern devices. It was challenging to point out the nanomaterials that are most appropriate for these devices. The numerical and experimental inspection of nanofluids by taking two different base solvents (water and ethylene glycol) was discussed in the study by Kazem et al. (2021). The study of solar thermal systems by considering phase change material was reported by Ndukwu et al. (2021). A review of nanotechnology applications in solar thermal systems was done in the study by Alktranee and Bencs (2021). The used nanomaterials are of various metals and oxides composed by them like ZnO, Al_2O_3, SiO_2, Fe, ND, Cu, and CuO. Despite this, there is another solid material commonly called carbon nanotubes (CNTs) (Bellos et al., 2018) which are further characterized as MWCNTs and SWCNTs, beneficial for thermal transport in SDs. These materials have very small diameter due to which these dissolved uniformly in regular liquids and enriched its thermal performance. The superior heat transport properties of nanoliquids strengthen their roots in various industries and are reported in the study by Zaharil (2021). The applications of nanotechnology under various circumstances for parabolic trough collectors are examined in the study by Ebrazeh and Sheikholeslami (2020).

The investigation of energy and entropy generation attracted researchers and scientists of the modern world. They thought that these features significantly alter due to the usage of new generation of regular liquids called nanoliquids. Earlier studies in this era were reported by Yejjer et al. (2017). The study of entropy for cylindrical pipes under the influence of nanofluids was deeply discussed by Ghanbarpour and Khodabandeh (2015). Recently, Shahzad et al. (2021) reported the dynamics of nanoliquids by Fe_3O_4 nanoparticles and found high thermal performance under certain flow conditions.

The influence of applied Lorentz forces on the flow behavior and heat transfer in the nanofluid in cavity was reported in by Benos and Sarris (2019). The dynamics of hybrid nanofluids (synthesized by aluminum and copper nanoparticles) with mixed convection and entropy analysis were examined by Li et al. (2021). Recently, Jamshed et al. (2021) explored the heat transfer inspection for second-grade fluid through a single phase model. Another imperative investigation of nanofluids' thermal performance by inducing the KKL model in the constitutive relations was reported by Kumar et al. (2021). The study for the nanoliquid composed by nickel ferrite and manganese ferrite by taking water as a base solvent was described by Song et al. (2021).

This study is organized to improve the heat transfer over a permeable surface coated with nanoliquid dispersed by γ-nanomaterial. The influences of solar thermal radiations and viscous dissipation will be imposed over a convective. Then a mathematical nanofluid model will be attained and treated numerically. After that, for actual effects of aforesaid physical quantities on the energy efficiency and drag forces will be plotted within the feasible region and discussed deeply.

2 THEORETICAL EXPERIMENT AND FLOW MODELING

2.1 Theoretical Experimental Setup

In this subsection, a proposed theoretical experimental setup is organized for PSTCS coated with new generation of conventional

TABLE 1 | Thermophysical values of $(\gamma Al_2O_3/H_2O)$nf.

Property	$\hat{\rho}$ (kg/m^3)	$\hat{\beta}$ (1/k)	$\hat{c}_p$ (J/Kg K)	$\hat{k}$ (W/mk)
$(H_2O)_{bf}$	998.3	20.05×10^{-5}	4182	0.60
$(Al_2O_3)_{np}$	3970	0.85×10^{-5}	765	40

liquids called nanoliquid. For energy efficiency of PSTCS, γAl_2O_3 nanoparticles, thermal radiations, and viscous dissipation are induced in the model of convective PSTCS. Another significant insight of drag forces on the wing of aircraft is also considered.

2.1.1 Motivational Aspects

- The shape of the aircraft wing imperatively alters the energy efficiency and drag forces, thus creating hindrance in the aircraft flight and resulting in energy loss. Therefore, PSTCS is used in the replacement of conventional PVC sheets.
- PSTCS has more energy storage capability because it is oriented in a cylindrical shape due to which its surface area is larger than conventional PVC.
- Solar aircraft make flight due to the storage of energy; hence, it is environment friendly and pollution free.
- The energy efficiency of PSTCS can be enhanced by coating its surface with new-generation fluids (nanofluids) diluted with γ-nanomaterial using thermal radiations, convective PSTCS, and viscous dissipation.
- Solar aircraft are human-friendly and economical due to their low manufacturing cost.

Figure 1B presents the setup of the theoretical experiment for PSTCS.

A schematic of the presence of imposed conditions, solar thermal radiations, and viscous dissipation is depicted in **Figure 1C**.

2.2 Nanofluid Flow Modeling

The mathematical modeling comprises the following information:

2.2.1 Empirical Nanofluid Correlations for $\gamma Al_2O_3/H_2O$

To improve the energy in the nanofluid, the following empirical correlations and their corresponding thermophysical values are utilized, and in the later stage, these will produce the flow model (Rashidi et al., 2016; Ahmed et al., 2017; Khan et al., 2017; Ahmed et al., 2018; Khan et al., 2020).

$$\left(\rho\widehat{C_p}\right)_{(\gamma Al_2O_3/H_2O)nf} = \left(\rho\widehat{C_p}\right)_{(H_2O)bf}\left[(1-\phi)+\frac{\phi\left(\rho\widehat{C_p}\right)_{(\gamma Al_2O_3)np}}{\left(\rho\widehat{C_p}\right)_{(H_2O)bf}}\right] \quad (1)$$

$$\hat{\rho}_{(\gamma Al_2O_3/H_2O)nf} = \left[(1-\phi)+\frac{\phi\hat{\rho}_{(\gamma Al_2O_3)np}}{\hat{\rho}_{(H_2O)bf}}\right]\hat{\rho}_{(H_2O)bf} \quad (2)$$

$$\left(\rho\widehat{\beta}\right)_{(\gamma Al_2O_3/H_2O)nf} = \left(\rho\widehat{\beta}\right)_{(H_2O)bf}\left[(1-\phi)+\frac{\phi\left(\rho\widehat{\beta}\right)_{(\gamma Al_2O_3)np}}{\left(\rho\widehat{\beta}\right)_{(H_2O)bf}}\right] \quad (3)$$

$$\hat{\mu}_{(\gamma Al_2O_3/H_2O)nf} = \hat{\mu}_{(H_2O)bf}\left(123\phi^2+7.3\phi+1\right) \quad (4)$$

$$\hat{k}_{(\gamma Al_2O_3/H_2O)nf} = \hat{k}_{(H_2O)bf}\left(4.97\phi^2+2.72\phi+1\right) \quad (5)$$

The thermophysical attributes of the used nanofluid are described in **Table 1** (Benos and Sarris, 2019; AdnanKhan et al., 2021; Gkountas et al., 2021; Hamid et al., 2021; Madhukesh et al., 2021; AdnanKhan et al., 2022).

2.2.2 Constitutive Flow Model

It is presumed that the flow is incompressible and steady, and has some viscosity. Furthermore, a uniform interaction of the nanoparticles and the base solvent is taken. The nanoparticles and the host liquid are in thermal equilibrium and no slip effects occur between them. Thus, in view of boundary layer approximation theory (BLAT) and presumed assumptions, the following models are obtained.

2.2.2.1 Conservation of Mass and Momentum

$$\breve{u}_x + \breve{v}_y = 0 \quad (6)$$

$$\breve{u}\breve{u}_x + \breve{v}\breve{u}_y\frac{\hat{\mu}_{(\gamma Al_2O_3/H_2O)nf}}{\hat{\rho}_{(\gamma Al_2O_3/H_2O)nf}}\breve{u}_{xx} - \frac{\hat{\mu}_{(\gamma Al_2O_3/H_2O)nf}}{\hat{\rho}_{(\gamma Al_2O_3/H_2O)nf}}\breve{u}k^{-1} = 0 \quad (7)$$

2.2.2.2 Conservation of Energy

$$\begin{aligned}&\breve{u}\breve{T}_x + \breve{v}\breve{T}_y - \frac{1}{\left(\rho\widehat{C_p}\right)_{(\gamma Al_2O_3/H_2O)nf}}\left(\hat{k}_{(\gamma Al_2O_3/H_2O)nf}\breve{T}_{yy}\right.\\&\left. - \frac{16\sigma^*T_\infty^3}{3k^*}\breve{T}_{yy} + \hat{\mu}_{(\gamma Al_2O_3/H_2O)nf}\left(\breve{u}_x\right)^2\right)\breve{u}\breve{T}_x + \mathrm{E}^*\left(\breve{u}\breve{T}_x\breve{u}_x\right.\\&\left. + \breve{v}\breve{T}_y\breve{v}_y + \breve{u}\breve{v}_x\breve{T}_y + \breve{v}\breve{u}_y\breve{T}_x + \breve{u}^2\breve{T}_{xx} + \breve{v}^2\breve{T}_{yy} + \breve{v}\breve{u}\breve{T}_{xy}\right)\\&= 0\end{aligned} \quad (8)$$

2.2.2.3 Imposed Conditions

The surface is subject to the following flow impositions:

$$\breve{u} = U_\infty + \mu_{nf}\left(\breve{u}_y\right),\ \breve{v} = \breve{v}_w,\ -k_g^*\left(\breve{T}_y\right) = h_g^*\left(\breve{T}_w - \breve{T}\right) \quad (9)$$

$$\breve{u} \to 0,\ \breve{T} \to \breve{T}_\infty \text{ at ambient location} \quad (10)$$

The velocity components are taken as $\boldsymbol{v} = (\breve{u}, \breve{v}, 0)$, $\breve{T}_w$ is the temperature at the surface, $\mathcal{E}^*$ is the relaxation time, $\breve{v}_w$ is the permeability, h_g^* is the coefficient of thermal transport, and $\breve{T}_\infty$ is the ambient temperature.

2.2.2.4 Similarity Equations

The following streaming function and similarity equations are introduced for the transformation of the dimensional model into a non-dimensional version:

$$\breve{u} = \Psi_y,\ \breve{v} = -\Psi_x, \quad (11)$$

$$\eta = \sqrt{\left(\frac{b}{\nu_{H_2O}}\right)}\,y,\ \Psi = \sqrt{\nu_{H_2O}bx}F,\ \beta = \frac{\breve{T}-\breve{T}_\infty}{\breve{T}_w-\breve{T}_\infty}. \quad (12)$$

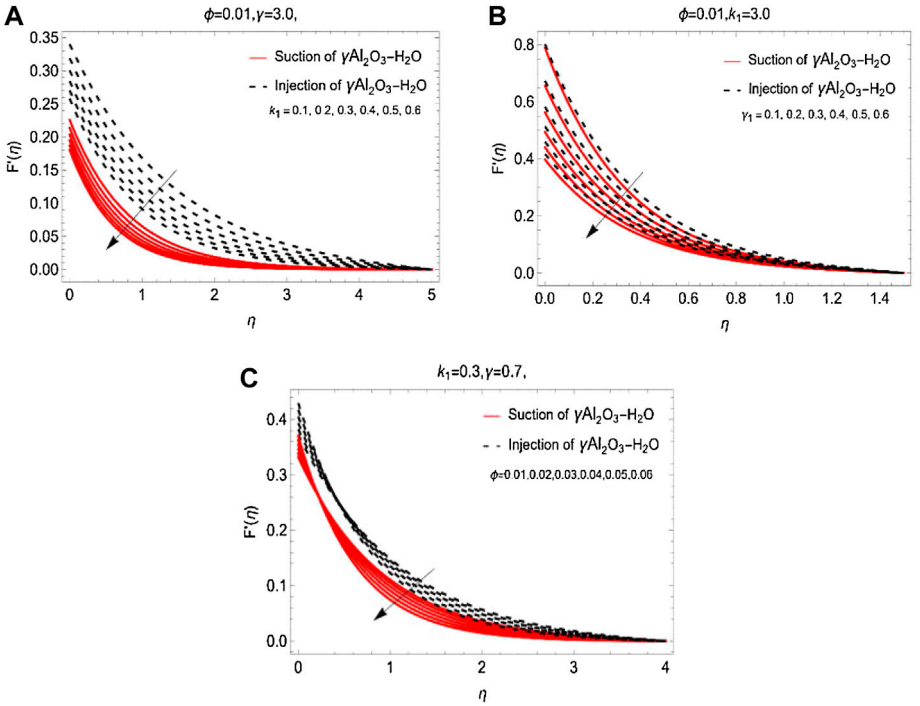

FIGURE 2 | Velocity profile for varying **(A)** k_1, **(B)** γ, and **(C)** ϕ.

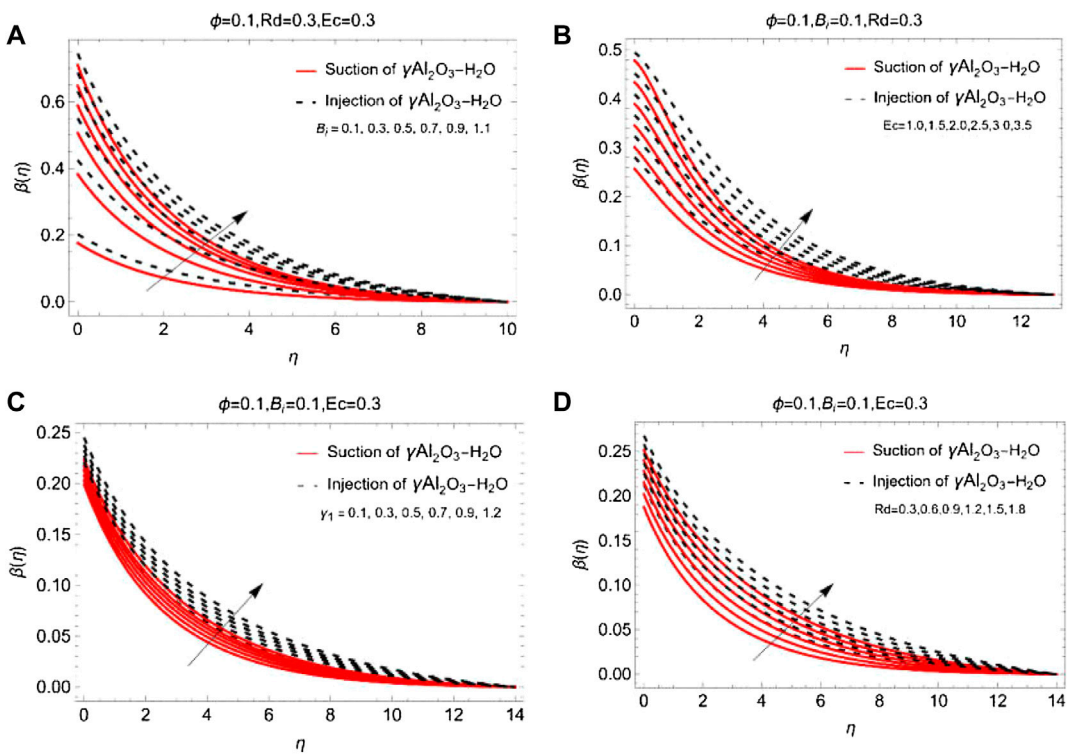

FIGURE 3 | Thermal distribution of the nanofluid for varying **(A)** B_1, **(B)** Ec, **(C)** γ, and **(D)** Rd.

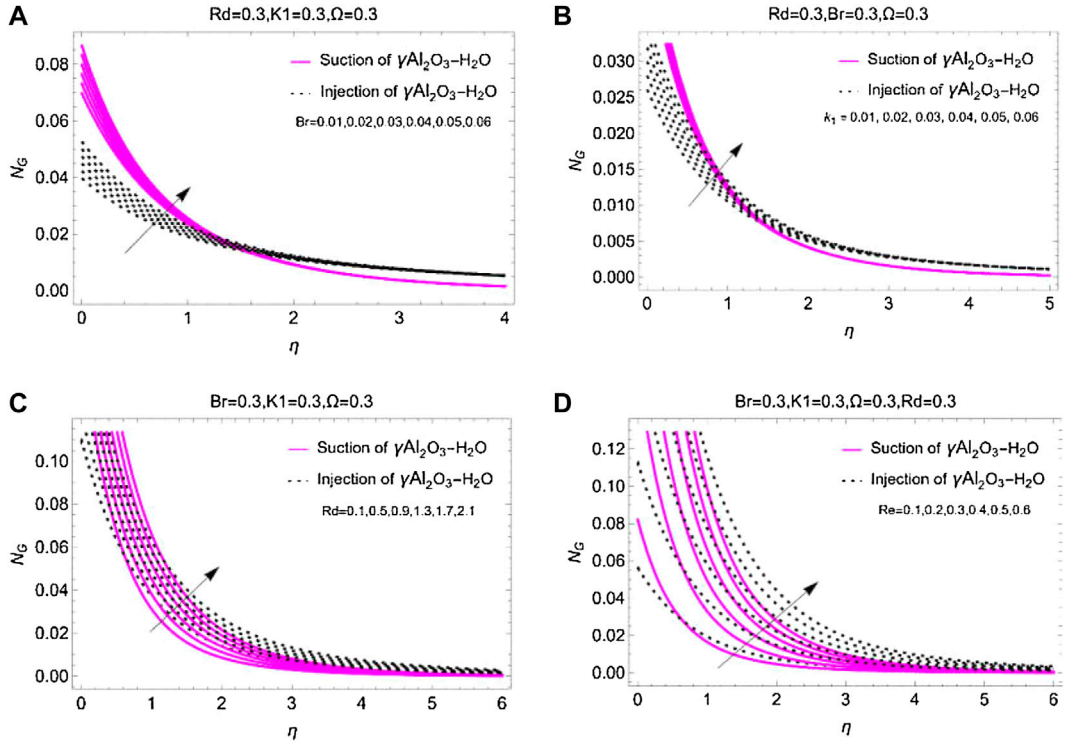

FIGURE 4 | Entropy generation investigation of the nanofluid for varying **(A)** Br, **(B)** k_1, **(C)** Rd, and **(D)** Re.

2.2.2.5 Final Version of the Model

By inducing the empirical correlations of the nanofluid, similarity equations, and impositions over the surface of the aircraft, the following version of the model is attained:

$$F''' + \frac{\left(123\phi^2 + 7.3\phi + 1\right)}{\left(\left(1-\phi\right) + \frac{\phi\rho_{(\gamma Al_2O_3)np}}{\rho_{(H_2O)bf}}\right)^{-1}}\left(FF'' - F'^2\right) - K_1F' = 0, \quad (13)$$

$$\beta''\left(1 + \frac{PrRd}{\left(4.97\phi^2 + 2.72\phi + 1\right)}\right) + \frac{\Pr\left(\left(1-\phi\right) + \frac{\phi\left(\rho C_p\right)_{(\gamma Al_2O_3)np}}{\left(\rho C_p\right)_{(H_2O)bf}}\right)}{\left(4.97\phi^2 + 2.72\phi + 1\right)}\left(F\beta' - F'\beta + \frac{Ec}{\left(123\phi^2 + 7.3\phi + 1\right)\left(\left(1-\phi\right) + \frac{\phi\left(\rho C_p\right)_{(\gamma Al_2O_3)np}}{\left(\rho C_p\right)_{(H_2O)bf}}\right)}F''^2 - \tilde{\varepsilon}\left(F'F\beta' + \beta'F^2\right)\right) = 0. \quad (14)$$

Subsequently, the new version of the imposed conditions is as follows:

$$F(0) = S,\ F'(0) = 1 + \frac{\gamma}{\left(123\phi^2 + 7.3\phi + 1\right)}F''(0),\ \beta'(0) = -B_1\left(1 - \beta(0)\right), \quad (15)$$

$$F'(\infty) \to 0,\ \beta(\infty) \to 0. \quad (16)$$

2.2.2.6 Modeling of Drag Forces

The drag forces significantly interfere in the efficiency and speed of the solar aircraft. Therefore, it is important to analyze the behavior of the shear stresses against different parameters. The following dimensional expression supports the shear stresses:

$$C_F = \frac{\tilde{\tau}_w}{\tilde{\rho}_{nf}\tilde{U}_w^2}. \quad (17)$$

With the help of shear stresses and nanoliquid empirical correlations, finally, the following version is attained:

$$C_F = \left[\frac{1}{\left(123\phi^2 + 7.3\phi + 1\right)\left(\left(1-\phi\right) + \frac{\phi\hat{\rho}_{(\gamma Al_2O_3)np}}{\hat{\rho}_{(H_2O)bf}}\right)}F''(\eta)\right]_{\eta=0}. \quad (18)$$

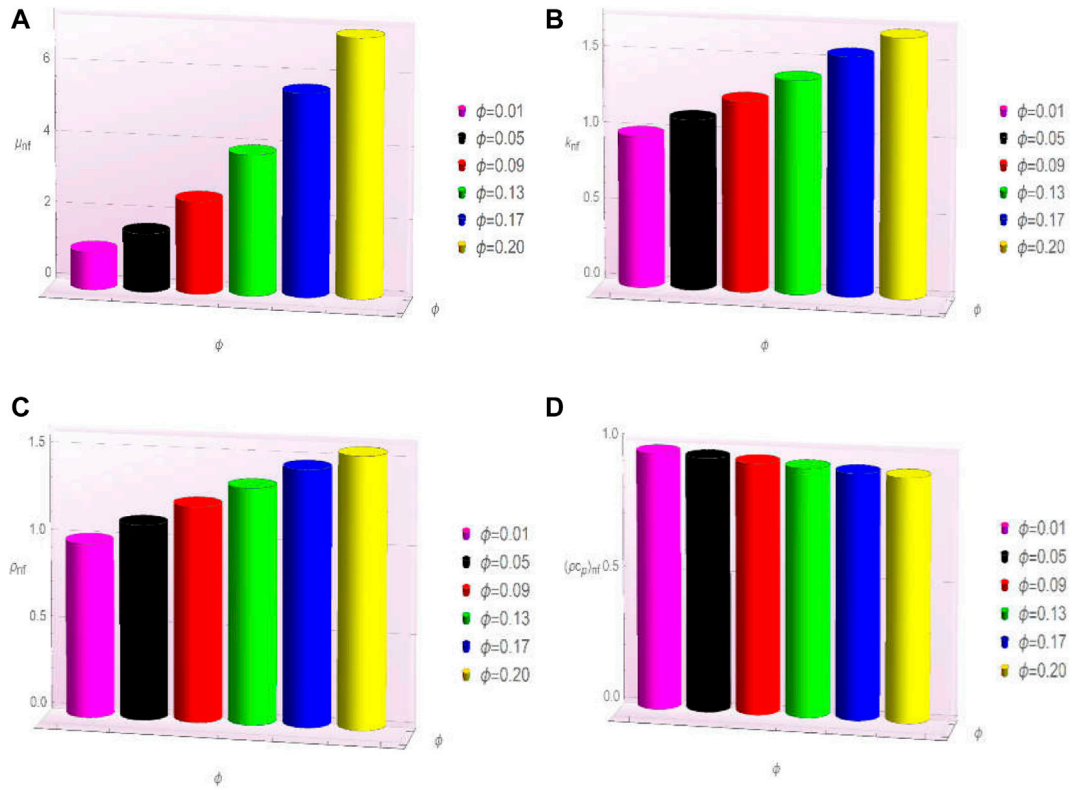

FIGURE 5 | Thermophysical featuring of the nanofluid for varying ϕ, **(A)** dynamic viscosity, **(B)** thermal conductivity, **(C)** effective density, and **(D)** heat capacity.

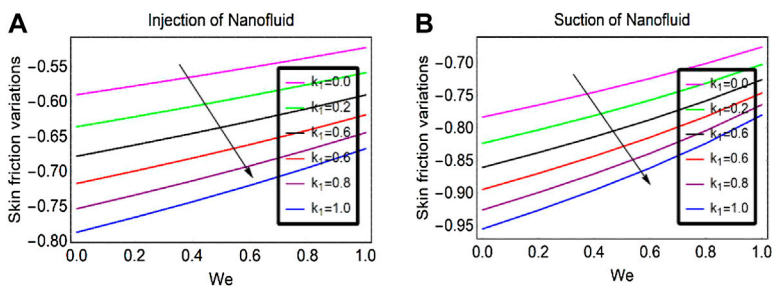

FIGURE 6 | Trends in the shear stresses in the nanofluid for varying **(A)** k_1 injection and **(B)** k_1 suction.

3 MATHEMATICAL ANALYSIS OF THE MODEL

To summarize the influences of various flow parameters, it is significant to analyze the corresponding mathematical model numerically. The modeled equations in engineering and other practical problems are coupled extremely nonlinearly on the bases of the flow scenario. The mathematical techniques based on approximate solutions are inadequate regarding the convergence due to which scientists and researchers prefer numerical treatment of the model. This technique is applicable when a higher-order system of ODEs is transformed into its subsystem of first-order ODEs. For this, a set of supporting transformations is required as below:

$$F = \breve{g}_1^*, F' = \breve{g}_2^*, F'' = \breve{g}_3^*, F''' = \breve{g}_3^{*'}, \beta' = \breve{g}_7^*, \beta' = \breve{g}_8^{*'}, \beta'' = \breve{g}_8^{*'}. \tag{19}$$

The model is then reduced in the following version:

$$\breve{g}_3^{*'} + \frac{\left(123\phi^2 + 7.3\phi + 1\right)}{\left(1 - \phi + \frac{\phi\hat{\rho}_{(\gamma Al_2O_3)np}}{\hat{\rho}_{(H_2O)bf}}\right)^{-1}}\left(\breve{g}_1^*\breve{g}_3^* - \breve{g}_3^{*2}\right) - K_1\breve{g}_2^* = 0, \tag{20}$$

$$\breve{g}_8^{'*}\left(1+\frac{PrRd}{(4.97\phi^2+2.72\phi+1)}\right)+\frac{\Pr\left((1-\phi)+\frac{\phi\left(\rho C_p\right)_{(\gamma Al_2O_3)np}}{\left(\rho C_p\right)_{(H_2O)bf}}\right)}{(4.97\phi^2+2.72\phi+1)}\left(\breve{g}_1^*\breve{g}_8^*-\breve{g}_2^*\breve{g}_7^*+\frac{Ec}{(123\phi^2+7.3\phi+1)\left((1-\phi)+\frac{\phi\left(\rho C_p\right)_{(\gamma Al_2O_3)np}}{\left(\rho C_p\right)_{(H_2O)bf}}\right)}\breve{g}_2^{*3}-\tilde{\mathrm{E}}\left(\breve{g}_2^*\breve{g}_1^*\breve{g}_8^*+\breve{g}_8^*\breve{g}_1^{*2}\right)\right)=0. \tag{21}$$

The transformed model is then coded in MATHEMATICA 10.0 and the graphical results furnished.

4 RESULTS WITH DISCUSSION

4.1 The Velocity Field

This subsection is devoted to analyzing the velocity over the surface against various flow parameters furnished in **Figure 2**.

The porosity effects on the velocity over a surface are presented in **Figure 2A** for both suction/injection of the fluid. The velocity drops significantly due to pores over the surface. Physically, more fluid particles drag to fill the pores due to which the frictional force becomes dominant and ultimately the motion declines. The prompt decrement is noticeable due to a lot of pores being present there, and, gradually, the motion decreases at ambient location. For the suction case, the fluid decreases abruptly because maximum fluid particles move over the surface to fill the space due to pores. For injecting fluid, the fluid moves quite rapidly over the surface.

Figures 2B,C show the fluid motion against slip effects γ and fraction factor ϕ. Due to the slip effects and by enhancing the fraction factor of the nanofluid, the velocity reduces prominently.

4.2 Thermal Distribution

Thermal behavior against extra convection (Biot number) from the surface is elaborated in **Figure 3A**. It is observed that the surface is heated convectively, and then a significant increase in the temperature occurs. Due to stronger effects at the surface, maximum rise in the temperature is noticed. Physically, the temperature of particles in the locality of the surface gain energy from the surface *via* conduction, and after that, these particles transfer energy to the rest of the particles *via* convection, which affects the wing temperature.

The effect of viscous dissipation, slip parameter, and solar thermal radiation on temperature is plotted in **Figures 3B–D**, respectively. From these, it is evident that energy storage could be enhanced in the presence of Ec, slip effects, and solar thermal radiations, which is ultimately beneficial for the aircraft. Furthermore, injection of the fluid significantly alters the thermal behavior.

4.3 Entropy Generation

Entropy optimization analysis in the light of varying flow quantities attained much interest from researchers and mechanical engineers. Therefore, this subsection is designed to observe the entropy behavior against B_r, K_1, Rd, and Re, respectively, in **Figures 4A–D**. From the analysis of these figures, it is noted that the entropy rises. However, injection of the fluid increases the entropy more rapidly than in the suction case.

4.4 Thermophysical Featuring of Empirical Correlations

Thermophysical values of the colloidal suspensions are key ingredients for thermal enhancement in the nanofluids. The trends in effective thermophysical values against the fraction factor are plotted in **Figure 5**. From the results, it is observed that effective density, thermal conductivity, and dynamic viscosity increase with the increase in the fraction factor. These are elaborated by **Figures 5A–C**. However, heat capacity drops by enhancing the nanomaterial fraction factor (**Figure 5D**).

4.5 Trends of Drag Forces

Shear drag forces over the surface are of great significance to enhance the efficiency of the aircraft during its flight. It is observed that the drag forces decrease prominently over the surface due to porosity. These results are presented in **Figures 6A,B**.

5 CONCLUDING REMARKS

This analysis concerns the heat transport inspection in $\gamma Al_2O_3 - H_2O$ nanofluid over a permeable convective surface. The model is properly obtained using similarity equations and empirical correlations of nanofluids and then solved numerically. The significant effects of velocity slip and porosity are incorporated in the flow model for convective surface. From the analysis, it was found that fluid motion decreases with an increase in porosity, slip parameter, and volumetric fraction (ϕ). The significant contribution of B_1 (Biot number) is reported, and optimum temperature variations near the surface are examined. The temperature of the nanofluid enhances stronger thermal radiations (Rd) and viscous dissipation effects (Ec), whereas a positive effect of temperature is observed against slip parameter. The entropy optimization improved against Brinkman and porosity parameters for the nanofluid. The nanofluids have better heat transport than regular liquids, and these could be very helpful in overcoming the heat transfer issues.

5.1 Future Perspectives

In future, the model could be extended for various types of nanolubricants and nanofluids by incorporating nonlinear thermal radiations, convective heat condition, second-order slip, and Joule heating effects. All these studies would be helpful in tackling problems related to heat transfer.

DATA AVAILABILITY STATEMENT

The numerical study is conducted and the data is given within the article. The raw data supporting the conclusion of this article will be made available by the authors, without undue reservation.

AUTHOR CONTRIBUTIONS

A and WA wrote the original draft. A and HJ performed the mathematical analysis. A and WA wrote the results and discussion. MM and SM revised the manuscript; rectified the grammatical mistakes and corrected; A, WA and IK validated the code.

REFERENCES

Abbe, G., and Smith, H. (2016). Technological Development Trends in Solar-powered Aircraft Systems. *Renew. Sustain. Energ. Rev.* 60, 770–783. doi:10.1016/j.rser.2016.01.053

AdnanKhan, U., Ashraf, W., Khan, U., Al-Johani, A. S., Ahmed, N., Mohyud-Din, S. T., et al. (2022). Impact of Freezing Temperature (Tfr) of Al_2O_3 and Molecular Diameter (H_2O)d on thermal Enhancement in Magnetized and Radiative Nanofluid with Mixed Convection. *Sci. Rep.* 12. doi:10.1038/s41598-021-04587-9

AdnanKhan, U., Khan, U., Ahmed, N., and Mohyud-Din, S. T. (2021). Enhanced Heat Transfer in H2O Inspired by Al_2O_3 and γAl_2O_3 Nanomaterials and Effective Nanofluid Models. *Adv. Mech. Eng.* 13 (5), 168781402110236. doi:10.1177/16878140211023604

Ahmed, N., AdnanKhan, U., and Mohyud-Din, S. T. (2018). A Theoretical Investigation of Unsteady Thermally Stratified Flow ofγAl_2O_3–H_2OandγAl_2O_3–$C_2H_6O_2$nanofluids through a Thin Slit. *J. Phys. Chem. Sol.* 119, 296–308. doi:10.1016/j.jpcs.2018.01.046

Ahmed, N., Khan, U. U., and Mohyud-Din, S. T. (2017). Influence of an Effective Prandtl Number Model on Squeezed Flow of γAl_2O_3 -H_2O and γAl_2O_3 -$C_2H_6O_2$ Nanofluids. *J. Mol. Liquids* 238, 447–454. doi:10.1016/j.molliq.2017.05.049

Alktranee, M., and Bencs, P. (2021). Applications of Nanotechnology with Hybrid Photovoltaic/Thermal Systems. *Jaes* 19, 1–15. doi:10.5937/jaes0-28760

Atiz, A. (2020). Comparison of Three Different Solar Collectors Integrated with Geothermal Source for Electricity and Hydrogen Production. *Int. J. Hydrogen Energ.* 45 (56), 31651–31666. doi:10.1016/j.ijhydene.2020.08.236

Bellos, E., Said, Z., and Tzivanidis, C. (2018). The Use of Nanofluids in Solar Concentrating Technologies: A Comprehensive Review. *J. Clean. Prod.* 196, 84–99. doi:10.1016/j.jclepro.2018.06.048

Benhadji Serradj, D. E., Sebitosi, A. B., and Fadlallah, S. O. (2021). Design and Performance Analysis of a Parabolic Trough Power Plant under the Climatological Conditions of Tamanrasset, Algeria. *Int. J. Environ. Sci. Technol.* 19, 3359–3376. doi:10.1007/s13762-021-03350-x

Benos, L., and Sarris, I. E. (2019). Analytical Study of the Magnetohydrodynamic Natural Convection of a Nanofluid Filled Horizontal Shallow Cavity with Internal Heat Generation. *Int. J. Heat Mass Transfer* 130, 862–873. doi:10.1016/j.ijheatmasstransfer.2018.11.004

Ebrazeh, S., and Sheikholeslami, M. (2020). Applications of Nanomaterial for Parabolic Trough Collector. *Powder Technol.* 375, 472–492. doi:10.1016/j.powtec.2020.08.005

Gao, X.-Z., Hou, Z.-X., Guo, Z., and Chen, X.-Q. (2015). Reviews of Methods to Extract and Store Energy for Solar-Powered Aircraft. *Renew. Sustain. Energ. Rev.* 44, 96–108. doi:10.1016/j.rser.2014.11.025

Ghanbarpour, M., and Khodabandeh, R. (2015). Entropy Generation Analysis of Cylindrical Heat Pipe Using Nanofluid. *Thermochim. Acta* 610, 37–46. doi:10.1016/j.tca.2015.04.028

Gkountas, A. A., Benos, L. T., Sofiadis, G. N., and Sarris, I. E. (2021). A Printed-Circuit Heat Exchanger Consideration by Exploiting an Al_2O_3-Water Nanofluid: Effect of the Nanoparticles Interfacial Layer on Heat Transfer. *Therm. Sci. Eng. Prog.* 22, 100818. doi:10.1016/j.tsep.2020.100818

Goudarzi, S., Shekaramiz, M., Omidvar, A., Golab, E., Karimipour, A., and Karimipour, A. (2020). Nanoparticles Migration Due to Thermophoresis and Brownian Motion and its Impact on Ag-MgO/Water Hybrid Nanofluid Natural Convection. *Powder Technol.* 375, 493–503. doi:10.1016/j.powtec.2020.07.115

Hamid, A., Naveen Kumar, R., Punith Gowda, R. J., Varun Kumar, R. S., Khan, S. U., Ijaz Khan, M., et al. (2021). Impact of Hall Current and Homogenous-Heterogenous Reactions on MHD Flow of GO-MoS_2/water (H_2O)-Ethylene Glycol $(C_2H_6O_2)$ Hybrid Nanofluid Past a Vertical Stretching Surface. *Waves in Random and Complex Media*, 1–18. doi:10.1080/17455030.2021.1985746

Jamshed, W., Nisar, K. S., Gowda, R. J. P., Kumar, R. N., and Prasannakumara, B. C. (2021). Radiative Heat Transfer of Second Grade Nanofluid Flow Past a Porous Flat Surface: a Single-phase Mathematical Model. *Physica Scripta* 96, 064006. doi:10.1088/1402-4896/abf57d

Kazem, H. A., Al-Waeli, A. H. A., Chaichan, M. T., and Sopian, K. (2021). Numerical and Experimental Evaluation of Nanofluids Based Photovoltaic/thermal Systems in Oman: Using Silicone-Carbide Nanoparticles with Water-Ethylene Glycol Mixture. *Case Stud. Therm. Eng.* 26, 101009. doi:10.1016/j.csite.2021.101009

Khan, U., AdnanAhmed, N., and Mohyud-Din, S. T. (2020). Surface thermal Investigation in Water Functionalized Al2O3 and γAl2O3 Nanomaterials-Based Nanofluid over a Sensor Surface. *Appl. Nanosci.* doi:10.1007/s13204-020-01527-3

Khan, U., Ahmed, N. N., and Mohyud-Din, S. T. (2017). 3D Squeezed Flow of γAl_2O_3-H_2O and γAl_2O_3-$C_2H_6O_2$ Nanofluids: A Numerical Study. *Int. J. Hydrogen Energ.* 42, 24620–24633. doi:10.1016/j.ijhydene.2017.07.090

Kumar, R. N., Suresha, S., Gowda, R. J. P., Megalamani, S. B., and Prasannakumara, B. C. (2021). Exploring the Impact of Magnetic Dipole on the Radiative Nanofluid Flow over a Stretching Sheet by Means of KKL Model. *Pramana* 95, 180. doi:10.1007/s12043-021-02212-y

Li, Y.-X., Khan, M. I., Gowda, R. J. P., Ali, A., Farooq, S., Chu, Y.-M., et al. (2021). Dynamics of Aluminum Oxide and Copper Hybrid Nanofluid in Nonlinear Mixed Marangoni Convective Flow with Entropy Generation: Applications to Renewable Energy. *Chin. J. Phys.* 73, 275–287. doi:10.1016/j.cjph.2021.06.004

Madhukesh, J. K., Kumar, R. N., Gowda, R. J. P., Prasannakumara, B. C., Ramesh, G. K., Khan, M. I., et al. (2021). Numerical Simulation of AA7072-AA7075/water-Based Hybrid Nanofluid Flow over a Curved Stretching Sheet with Newtonian Heating: A Non-fourier Heat Flux Model Approach. *J. Mol. Liquids* 335, 116103. doi:10.1016/j.molliq.2021.116103

Malan, A., and Kumar, K. R. (2021). A Comprehensive Review on Optical Analysis of Parabolic Trough Solar Collector. *Sustainable Energ. Tech. Assessments* 46, 101305.

Mwesigye, A., and Yılmaz, I. H. (2020). Thermal and Thermodynamic Benchmarking of Liquid Heat Transfer Fluids in a High Concentration Ratio Parabolic Trough Solar Collector System. *J. Mol. Liquids* 319, 114151. doi:10.1016/j.molliq.2020.114151

Ndukwu, M. C., Bennamoun, L., and Simo-Tagne, M. (2021). Reviewing the Exergy Analysis of Solar Thermal Systems Integrated with Phase Change Materials. *Energies* 14, 724. doi:10.3390/en14030724

Rashidi, M. M., Vishnu Ganesh, N., Abdul Hakeem, A. K., Ganga, B., and Lorenzini, G. (2016). Influences of an Effective Prandtl Number Model on Nano Boundary Layer Flow of γ Al_2O_3–H_2O and γ Al_2O_3–$C_2H_6O_2$ over a Vertical Stretching Sheet. *Int. J. Heat Mass Transfer* 98, 616–623. doi:10.1016/j.ijheatmasstransfer.2016.03.006

Rezaeian, M., Shafiey Dehaj, M., Zamani Mohiabadi, M., Salarmofrad, M., and Shamsi, S. (2021). Experimental Investigation into a Parabolic Solar Collector with Direct Flow Evacuated Tube. *Appl. Therm. Eng.* 189, 116608. doi:10.1016/j.applthermaleng.2021.116608

Shahzad, F., Jamshed, W., Sajid, T., Nisar, K. S., and Eid, M. R. (2021). Heat Transfer Analysis of MHD Rotating Flow of Fe_3O_4 Nanoparticles through a Stretchable Surface. *Commun. Theor. Phys.* 73, 075004. doi:10.1088/1572-9494/abf8a1

Song, Y.-Q., Khan, M. I., Qayyum, S., Gowda, R. J. P., Kumar, R. N., Prasannakumara, B. C., et al. (2021). Physical Impact of Thermo-Diffusion and Diffusion-Thermo on Marangoni Convective Flow of Hybrid Nanofluid ($MnZiFe_2O_4$-$NiZnFe_2O_4$-H_2o) with Nonlinear Heat Source/sink and Radiative Heat Flux. *Mod. Phys. Lett. B* 35, 2141006–2141022. doi:10.1142/S0217984921410062

Wu, J., Han, Y., and Hou, H. (2020). A New Solar Share Evaluation Method of Solar Aided Power Generation (SAPG) System by Tracing Exergy Flows and Allocating Exergy Destruction. *Solar Energy* 198, 542–554. doi:10.1016/j.solener.2020.01.059

Yejjer, O., Kolsi, L., Aich, W., Al-Rashed, A. A. A. A., Borjini, M. N., and Ben Aissia, H. (2017). Study of Three-Dimensional Natural Convection and Entropy Generation in an Inclined Solar Collector Equipped with Partitions. *Heat Trans. Asian Res.* 46, 1312–1326. doi:10.1002/htj.21275

Zaharil, H. A. (2021). An Investigation on the Usage of Different Supercritical Fluids in Parabolic Trough Solar Collector. *Renew. Energ.* 168, 676–691. doi:10.1016/j.renene.2020.12.090

Zayed, M. E., Zhao, J., Li, W., Elsheikh, A. H., Elaziz, M. A., Yousri, D., et al. (2021). Predicting the Performance of Solar Dish Stirling Power Plant Using a Hybrid Random Vector Functional Link/chimp Optimization Model. *Solar Energy* 222, 1–17. doi:10.1016/j.solener.2021.03.087

Zhu, X., Guo, Z., and Hou, Z. (2014). Solar-powered Airplanes: A Historical Perspective and Future Challenges. *Prog. Aerospace Sci.* 71, 36–53. doi:10.1016/j.paerosci.2014.06.003

Conflict of Interest: The authors declare that the research was conducted in the absence of any commercial or financial relationships that could be construed as a potential conflict of interest.

NOMENCLATURE

$(\breve{u}, \breve{v})$ velocity components along the coordinate axes [m/s]

(x, y) coordinate axes

$\breve{T}$ temperature [Kelvin]

U_∞ velocity at free stream [m/s]

$\breve{T}_\infty$ ambient temperature [Kelvin]

$\breve{T}_w$ surface temperature [Kelvin]

$(\widehat{C_p})_{(\gamma Al_2O_3/H_2O)nf}$ nanofluid heat capacity [J/K]

$(\widehat{C_p})_{(H_2O)bf}$ heat capacity of base solvent [J/K]

$(\widehat{C_p})_{(\gamma Al_2O_3)np}$ heat capacity of nanoparticles [J/K]

ϕ volumetric fraction

$\hat{\rho}_{(\gamma Al_2O_3/H_2O)nf}$ density of nanofluid [kg/m^3]

$\hat{\rho}_{(\gamma Al_2O_3)np}$ density of nanoparticles [kg/m^3]

$\hat{\rho}_{(H_2O)bf}$ density of base solvent [kg/m^3]

$\hat{\mu}_{(\gamma Al_2O_3/H_2O)nf}$ dynamic viscosity [kg/ms]

$\hat{\mu}_{(H_2O)bf}$ dynamic viscosity of water [kg/ms]

$\hat{k}_{(\gamma Al_2O_3/H_2O)nf}$ thermal conductivity of nanofluid [W/mK]

$\hat{k}_{(H_2O)bf}$ thermal conductivity of water [W/mK]

$\hat{k}_{(Al_2O_3)}$ thermal conductivity of nanoparticles [W/mK]

h_g^* thermal transport coefficient

Ψ stream function

Pr Prandtl number

Rd Thermal radiation parameter

Ec Eckert number

S Suction/inject parameter

γ velocity slip parameter

B_1 Biot number

$F'(\eta)$ dimensionless velocity

$\beta(\eta)$ dimensionless temperature